JHEP01(2011)069

# Double-lepton polarization asymmetries and branching ratio in $B \to K_0^*(1430)l^+l^-$ transition from universal extra dimension model

**B.B. Şirvanlı,**[a] **K. Azizi,**[b] **and Y. Ipekoğlu**[c]

[a]*Department of Physics, Faculty of Arts and Science, Gazi University,*
*Teknikokullar, 06100 Ankara, Turkey*

[b]*Physics Division, Faculty of Arts and Sciences, Doğuş University, Acıbadem-Kadıköy,*
*34722 Istanbul, Turkey*

[c]*Physics Department, Middle East Technical University,*
*Cankaya, 06531 Ankara, Turkey*

*E-mail:* bbelma@gazi.edu.tr, kazizi@dogus.edu.tr, ipekoglu@metu.edu.tr

ABSTRACT: We investigate the $B \to K_0^*(1430)l^+l^-$ transition in the Applequist-Cheng-Dobrescu model in the presence of a universal extra dimension. In particular, we calculate double lepton polarization asymmetries and branching ratio related to this channel and compare the obtained results with the predictions of the standard model. Our analysis of the considered observables in terms of radius $R$ of the compactified extra-dimension as the new parameter of the model show a considerable discrepancy between the predictions of two models in low $\frac{1}{R}$ values.

# Contents

## 1 Introduction

The $B \rightarrow K_0^*(1430)l^+l^-$ transition proceeds via flavor changing neutral current (FCNC) transition of $b \rightarrow sl^+l^-$ at loop level. Such transition can be used in constraining the standard model (SM) parameters as well as gaining useful information about new physics effects such as extra dimensions, fourth generation of the quarks, supersymmetric particles and light dark matter , etc. The SM of particle physics can explain almost all known collider data and is in perfect agreement with the experiments so far. However, there are some problems such as, the origin of the matter in the universe, gauge and fermion mass hierarchy, number of generations, matter- antimatter asymmetry, unification, quantum gravity and so on, which can not explained by the SM. Hence, the SM can be thought to be a low energy manifestation of some underlying more fundamental theory or, to solve the aforementioned problems, some alternative theories are needed.

The extra dimension (ED) model with a flat metric [1–4] or with small compactification radius is one of the alternative theories. The ED is categorized as universal extra dimension (UED), where the SM fields containing gauge bosons and fermions can propagate in the extra dimensions and non-universal extra dimension (NUED), where the gauge bosons propagate into the extra dimensions, but the fermions are confined to the usual three spatial dimensions ($D_3$ brane). The simplest example of the UED where just a single universal extra dimension is taken into account is called the Appelquist, Cheng and Dobrescu (ACD) model [5]. Compared to the SM, this model has one extra parameter called compactification radius, $R$. Hence, this model is a minimal extension of the SM in $4 + 1$ dimensions with the extra dimension compactified to the orbifold $S^1/Z_2$ and the fifth coordinate, $y$ running between 0 and $2\pi R$, and $y = 0$ and $y = \pi R$ are fixed points of the orbifold. The zero modes of fields propagating in the extra dimension correspond the SM particles. The higher modes with momentum propagating in the extra dimension are called Kaluza-Klein (KK) modes. The mass of KK particles and interactions among them and also their interactions with the SM particles are explained in terms of the compactification scale, $1/R$. One of the important properties of the ACD model is conservation of the KK parity, $(-1)^{KK \ number}$

(for details about the method see also [6–9]). Such conservation entails the absence of tree level contributions of KK mods to processes occur at low energies, $\mu \ll \frac{1}{R}$, requiring the production of a single KK particle from the interaction of th SM particles. This allows us to use accurate electroweak measurements to supply a lower bound to the compactification scale, $\frac{1}{R} \geq (250-300)\ GeV$ [9, 10]. As these excitations can affect the loop level processes, especially FCNC transitions, investigation of $B \to K_0^*(1430)l^+l^-$ channel in the framework of the ACD model can be useful for constraining the parameters related to this new physics scenario.

The ACD model has been applied widely to calculate many observables related to the radiative and semileptonic decays of hadrons (for some of them see for example [6–9, 11–14]. In the present work, we calculate double lepton polarization asymmetries and branching ratio related to the rare semileptonic $B \to K_0^*(1430)l^+l^-$ transition in terms of radius $R$ of the compactified extra-dimension as the new parameter of the model in the framework of the ACD model. We compare the obtained results with the predictions of the standard model. The outline of the paper is as follows. In section 2, we introduce the effective Hamiltonian responsible for the $b \to sl^+l^-$ transition. Using the effective Hamiltonian, we obtain the branching ratio as well as the various related double lepton polarization asymmetries in terms of form factors also in this section. Using the fit parametrization of the form factors obtained using QCD sum rules, we numerically analyze the considered observables in section 3. This section also includes a comparison of the results obtained in ACD model with that of predicted by the SM and our discussions.

## 2 Branching ratio and double lepton polarization asymmetries in $B \to K_0^* l^+ l^-$ transition

At quark level, the $B \to K_0^* l^+ l^-$ transition proceed via FCNC transition of the $b \to sl^+l^-$. The effective Hamiltonian responsible for this transition at quark level can be written as:

$$\mathcal{H}^{\text{eff}} = \frac{G_F \alpha_{\text{em}} V_{tb} V_{ts}^*}{2\sqrt{2}\pi} \left[ C_9^{\text{eff}} \bar{s}\gamma_\mu(1-\gamma_5)b\, \bar{\ell}\gamma^\mu\ell + C_{10}\bar{s}\gamma_\mu(1-\gamma_5)b\, \bar{\ell}\gamma^\mu\gamma_5\ell \right.$$
$$\left. - 2m_b C_7^{\text{eff}} \frac{1}{q^2} \bar{s}i\sigma_{\mu\nu}q^\nu(1+\gamma_5)b\, \bar{\ell}\gamma^\mu\ell \right], \tag{2.1}$$

where $G_F$ is the Fermi constant, $\alpha_{\text{em}}$ is the fine structure constant at Z mass scale, $V_{ij}$ are elements of the Cabibbo-Kobayashi-Maskawa (CKM) matrix and $C_7^{\text{eff}}$, $C_9^{\text{eff}}$ and $C_{10}$ are the Wilson coefficients, which are the main source of the deviation of the ACD and SM models predictions on the considered observables. The Wilson coefficients can be expressed in terms of the periodic functions, $F(x_t, 1/R)$ with $x_t = m_t^2/M_W^2$ and $m_t$ being the top quark mass. Similar to the mass of the KK particles described in terms of the zero modes ($n = 0$) correspond to the ordinary particles of the SM and extra parts coming from the ACD model, the functions, $F(x_t, 1/R)$ are also written in terms of the corresponding SM functions,

| | $f_i(0)$ | $a_i$ | $b_i$ |
|---|---|---|---|
| $f_+$ | $0.31 \pm 0.08$ | $0.81$ | $-0.21$ |
| $f_-$ | $-0.31 \pm 0.07$ | $0.80$ | $-0.36$ |
| $f_T$ | $-0.26 \pm 0.07$ | $0.41$ | $-0.32$ |

**Table 1**. Parameters entering the fit parametrization of the form factors for $B \to K_0^* \ell^+ \ell^-$ transition.

$F_0(x_t)$ and extra parts which are functions of the compactification factor, $1/R$, i.e.,

$$F(x_t, 1/R) = F_0(x_t) + \sum_{n=1}^{\infty} F_n(x_t, x_n), \tag{2.2}$$

where $x_n = \dfrac{m_n^2}{M_W^2}$ and $m_n = \dfrac{n}{R}$. The Glashow-Illiopoulos-Maiani (GIM) mechanism guarantees the finiteness of the functions, $F(x_t, 1/R)$ and satisfies the condition, $F(x_t, 1/R) \to F_0(x_t)$, when $R \to 0$. As far as $1/R$ is taken in the order of a few hundreds of $GeV$, these functions and as a result, the Wilson coefficients differ considerably from the SM values. For explicit expressions of the Wilson coefficients in ACD model see [6, 7, 9].

To obtain the amplitude for the $B \to K_0^* l^+ l^-$ transition, we need to sandwich the effective Hamiltonian between the initial and final states. As a result of this procedure, the matrix elements, $\langle K_0^* | \bar{s}\gamma_\mu (1 - \gamma_5)b | B \rangle$ and $\langle K_0^* | \bar{s}i\sigma_{\mu\nu}q^\mu (1 + \gamma_5)b | B \rangle$ are obtained which should be calculated in terms of some form factors. Due to the parity considerations, the vector $(\bar{s}\gamma_\mu b)$ and tensor $(\bar{s}i\sigma_{\mu\nu}q^\nu b)$ parts of the transition current have no contributions. The matrix elements related to the axial-vector and pseudo-tensor parts of the transition currents are parameterized in terms of the form factors, $f_+$, $f_-$, and $f_T$ in the following way:

$$\langle K_0^*(p') | \bar{s}\gamma_\mu \gamma_5 b | B(p) \rangle = f_+(q^2)\mathcal{P}_\mu + f_-(q^2)q_\mu \tag{2.3}$$

$$\langle K_0^*(p') | \bar{s}i\sigma_{\mu\nu}q^\mu \gamma_5 b | B(p) \rangle = \frac{f_T(q^2)}{m_B + m_{K_0^*}}[\mathcal{P}_\mu q^2 - (m_B^2 - m_{K_0^*}^2)q_\mu] \tag{2.4}$$

where $\mathcal{P} = p + p'$ and $q = p - p'$. These form factors have been calculated in [16] in the framework of the three-point QCD sum rules. The fit parametrization of the form factors is given as:

$$f_i(\hat{s}) = \frac{f_i(0)}{1 - a_i\hat{s} + b_i\hat{s}^2}, \tag{2.5}$$

where $i = +, -$ or $T$ and $\hat{s} = q^2/m_B^2$. The values of the parameters $f_i(0)$, $a_i$ and $b_i$ are given in table 1.

Now, we proceed to calculate the differential decay rate for the considered transition. Using the amplitude and definition of the transition matrix elements in terms of the form

factors, we get the following expression for the $1/R$-dependent differential decay rate:

$$\frac{d\Gamma}{d\hat{s}}(\hat{s}, 1/R) = \frac{G^2 \alpha_{\text{em}}^2 m_B^5}{3072\pi^5} |V_{tb}V_{ts}^*|^2 v\sqrt{\lambda(1, \hat{m}_{K_0^*}^2, \hat{s})} \Bigg\{ \Bigg[ \Bigg| C_9^{\text{eff}}(\hat{s}, 1/R)f_+(\hat{s}) +$$

$$+\frac{2\hat{m}_b}{1 + \hat{m}_{K_0^*}} C_7^{\text{eff}}(1/R)f_T(\hat{s}) \Bigg|^2 + |C_{10}(1/R)f_+(\hat{s})|^2 \Bigg] (3 - v^2)\lambda(1, \hat{m}_{K_0^*}^2, \hat{s}) + \qquad (2.6)$$

$$+12\hat{m}_\ell^2 \Big[ (2 + 2\hat{m}_{K_0^*}^2 - \hat{s})|f_+(\hat{s})|^2 + 2(1 - \hat{m}_{K_0^*}^2)\text{Re}[f_+(\hat{s})f_-^*(\hat{s})] + \hat{s}\,|f_-(\hat{s})|^2 \Big] |C_{10}(1/R)|^2 \Bigg\},$$

where, $v = \sqrt{1 - \frac{4\hat{m}_\ell^2}{\hat{s}}}$, $\hat{m}_b = \frac{m_b}{m_B}$, $\hat{m}_\ell = \frac{m_\ell}{m_B}$, $\hat{m}_{K_0^*} = \frac{m_{K_0^*}}{m_B}$ and $\lambda(a, b, c) = a^2 + b^2 + c^2 - 2ab - 2ac - 2bc$ is the usual triangle function. Integrating out the above equation in the allowed physical region of the $\hat{s}$ $(4\hat{m}_\ell^2 \leq \hat{s} \leq (1 - \hat{m}_{K_0^*})^2)$, one can get the $1/R$-dependent total decay rate and branching ratio.

At the end of this section, we focus our attention to obtain the double-lepton polarization asymmetries. We calculate these asymmetries when polarizations of both leptons simultaneously are considered. Using the definitions of the double-lepton polarization asymmetries expressed in [17–19], we obtain the $1/R$-dependent polarizations,

$$P_{LL}(\hat{s}, 1/R) = \frac{-4m_B^2}{3\Delta(\hat{s}, 1/R)} Re[-24m_B^2\hat{m}_l^2(1 - \hat{r}_{K_0^*})C^*D + \lambda m_B^2(1 + v^2)|A|^2 \qquad (2.7)$$

$$- 12m_B^2\hat{m}_l^2\hat{s}|D|^2 + m_B^2|C|^2(2\lambda - (1 - v^2)(2\lambda + 3(1 - \hat{r}_{K_0^*})^2))], \qquad (2.8)$$

$$P_{LN}(\hat{s}, 1/R) = \frac{-4\pi m_B^3\sqrt{\lambda\hat{s}}}{\hat{s}\Delta(\hat{s}, 1/R)} Im[-m_B\hat{m}_l\hat{s}A^*D - m_B\hat{m}_l(1 - \hat{r}_{K_0^*})A^*C], \qquad (2.9)$$

$$P_{NL}(\hat{s}, 1/R) = -P_{LN}(\hat{s}, 1/R), \qquad (2.10)$$

$$P_{LT}(\hat{s}, 1/R) = \frac{4\pi m_B^3\sqrt{\lambda\hat{s}}}{\hat{s}\Delta(\hat{s}, 1/R)} Re[m_B\hat{m}_l v(1 - \hat{r}_{K_0^*})|C|^2 + m_B\hat{m}_l v\hat{s}C^*D], \qquad (2.11)$$

$$P_{TL}(\hat{s}, 1/R) = P_{LT}(\hat{s}, 1/R), \qquad (2.12)$$

$$P_{NT}(\hat{s}, 1/R) = -\frac{8m_B^2 v}{3\Delta(\hat{s}, 1/R)} Im[2\lambda m_B^2 A^*C], \qquad (2.13)$$

$$P_{TN}(\hat{s}, 1/R) = -P_{NT}(\hat{s}, 1/R), \qquad (2.14)$$

$$P_{TT}(\hat{s}, 1/R) = \frac{4m_B^2}{3\Delta(\hat{s}, 1/R)} Re[-24m_B^2\hat{m}_l^2(1 - \hat{r}_{K_0^*})C^*D - \lambda m_B^2(1 + v^2)|A|^2 - 12m_B^2\hat{m}_l^2\hat{s}|D|^2$$

$$+ m_B^2|C|^2\{2\lambda - (1 - v^2)(2\lambda + 3(1 - \hat{r}_{K_0^*})^2)\}], \qquad (2.15)$$

$$P_{NN}(\hat{s}, 1/R) = \frac{4m_B^2}{3\Delta(\hat{s}, 1/R)} Re[24m_B^2\hat{m}_l^2(1 - \hat{r}_{K_0^*})C^*D - \lambda m_B^2(3 - v^2)|A|^2 + 12m_B^2\hat{m}_l^2\hat{s}|D|^2$$

$$+ m_B^2|C|^2\{2\lambda - (1 - v^2)(2\lambda - 3(1 - \hat{r}_{K_0^*})^2)\}] \qquad (2.16)$$

where, $L$, $N$ and $T$ stand for the longitudinal, normal and transversal polarizations, re-

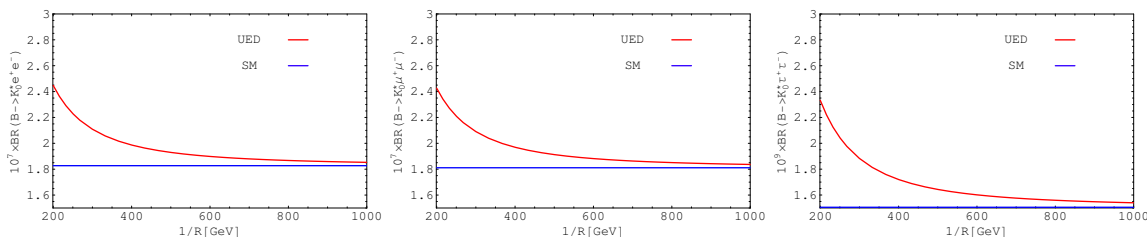**Figure 1**. The dependence of the branching ratio for $B \to K_0^* l^+ l^-$ on the compactification factor, $1/R$ for different leptons.

spectively, $\hat{r}_{K_0^*} = \hat{m}_{K_0^*}^2$, $\lambda = \lambda(1, \hat{r}_{K_0^*}, \hat{s})$ and

$$\Delta(\hat{s}, 1/R) = \frac{4m_B^2}{3} Re[24m_B^2 \hat{m}_l^2 (1 - \hat{r}_{K_0^*}) D^* C + \lambda m_B^2 (3 - v^2)|A|^2 + 12m_B^2 \hat{m}_l^2 \hat{s} |D|^2$$
$$+ m_B^2 |C|^2 \{2\lambda - (1 - v^2)(2\lambda - 3(1 - \hat{r}_{K_0^*})^2)\}]$$

$$A = A(\hat{s}, 1/R) = 2C_9^{\text{eff}}(\hat{s}, 1/R) f_+(\hat{s}) - 4C_7^{\text{eff}}(1/R)(m_b + ms) \frac{f_T(\hat{s})}{m_B + m_{K_0^*}},$$

$$B = B(\hat{s}, 1/R) = 2C_9^{\text{eff}}(\hat{s}, 1/R) f_-(\hat{s}) + 4C_7^{\text{eff}}(1/R)(m_b + ms) \frac{f_T(\hat{s})}{(m_B + m_{K_0^*})\hat{s}m_B^2}(m_B^2 - m_{K_0^*}^2),$$

$$C = C(\hat{s}, 1/R) = 2C_{10}(1/R) f_+(\hat{s}),$$

$$D = D(\hat{s}, 1/R) = 2C_{10}(1/R) f_-(\hat{s}) . \tag{2.17}$$

## 3 Numerical results

In this section, we numerically analyze the expressions of the branching ratio and double-lepton polarization asymmetries and discuss their dependence and sensitivity on the compactification factor, $1/R$. Some input parameters of the SM used in the numerical analysis are: $m_t = 167 \, GeV$, $m_W = 80.4 \, GeV$, $m_Z = 91.18 \, GeV$, $m_c = 1.46 \, GeV$, $m_b = 4.8 \, GeV$, $m_u = 0.005 \, GeV$, $m_B = 5.28 \, GeV$, $m_{K_0^*} = 1.425 \, GeV$, $sin^2\theta_W = 0.23$, $\alpha_{\text{em}} = \frac{1}{137}$, $\alpha_s(m_Z) = 0.118$, $|V_{tb}V_{ts}^*| = 0.041$, $G_F = 1.167 \times 10^{-5} \, GeV^{-2}$, $m_e = 5.1 \times 10^{-4} \, GeV$, $m_\mu = 0.109 \, GeV$, $m_\tau = 1.784 \, GeV$, and $\tau_B = 1.525 \times 10^{-12} s$. As we previously mentioned, the branching ratio is obtained integrating the differential decay rate over $\hat{s}$ in the physical region of the square of the momentum transfered, $q^2$, hence the obtained expression for the branching ration only depends on the compactification factor. In figure 1, we present the dependence branching ratio of the $B \to K_0^* l^+ l^-$ transition on compactification parameter, $1/R$ in the interval, $200 \, GeV \leq 1/R \leq 1000 \, GeV$ for different leptons.

From this figure, we deduce the following results:

- There are considerable discrepancies between the predictions of the ACD and SM models for low values of the compactification factor, $1/R$. As $1/R$ increases, the difference between the predictions of the two models tends to diminish. The result of ACD approaches the result of SM for higher values of $1/R$ ($1/R \simeq 1000 \, GeV$). Such a discrepancy at low values of $1/R$ can be a signal for the existence of extra dimensions.
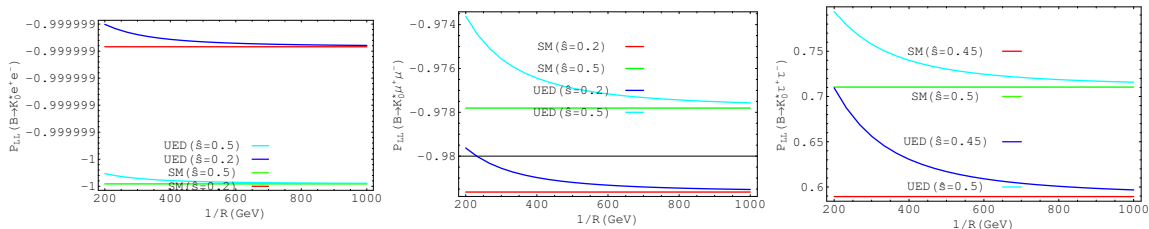
**Figure 2**. The dependence of the $P_{LL}$ polarization in two models for $B \to K_0^* l^+ l^-$ on the compactification factor, $1/R$ at different fixed values of $\hat{s}$ and different leptons.
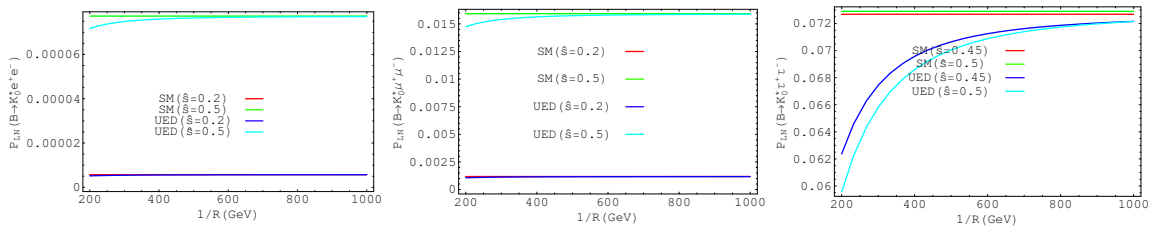


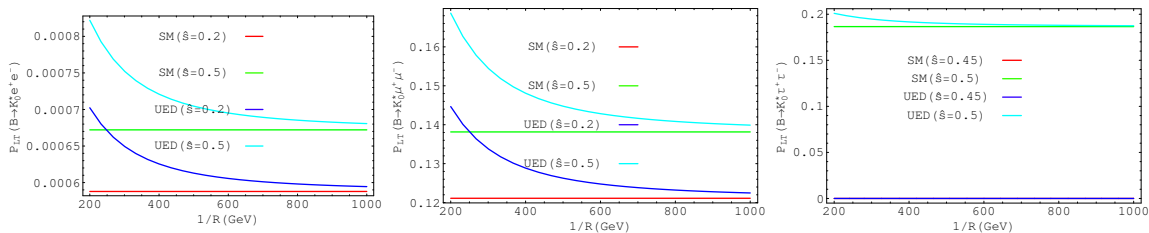**Figure 3**. The same as figure 2, but for $P_{LN}$ polarization.



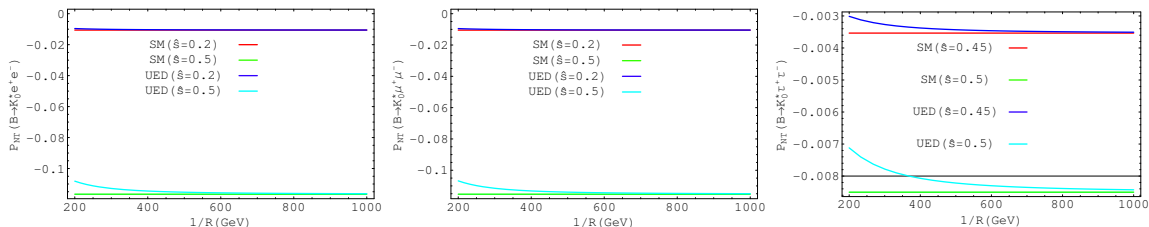**Figure 4**. The same as figure 2, but for $P_{LT}$ polarization.



**Figure 5**. The same as figure 2, but for $P_{NT}$ polarization.

- As it is expected, an increase in the lepton mass results in a decrease in the branching ratio. The branching ratios for the $e$ and $\mu$ are approximately the same.

- The order of magnitude of the branching ratio, specially for the $e$ and $\mu$, depicts a possibility to study such channels at the LHC.

Now, we proceed to show the results of the double-lepton polarization asymmetries. As it is clear from their explicit expressions, they depend on both the compactification factor, $1/R$ and the $\hat{s}$. The dependence of different polarization asymmetries on the compactification
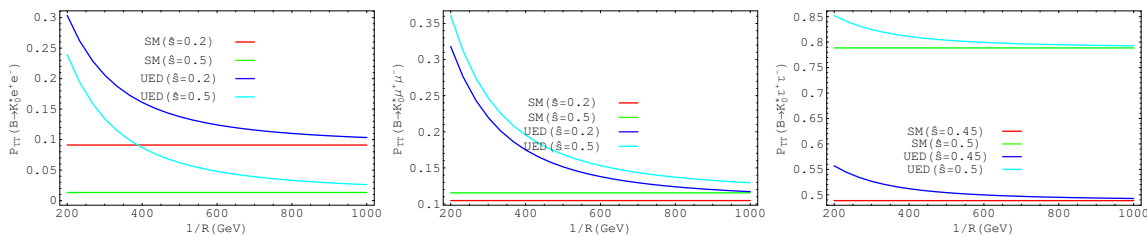
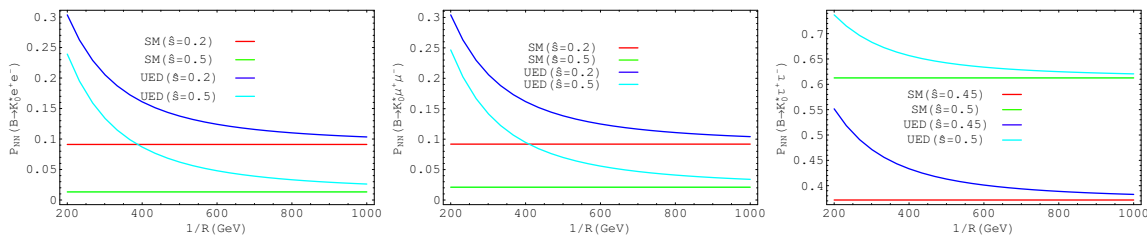**Figure 6**. The same as figure 2, but for $P_{TT}$ polarization.



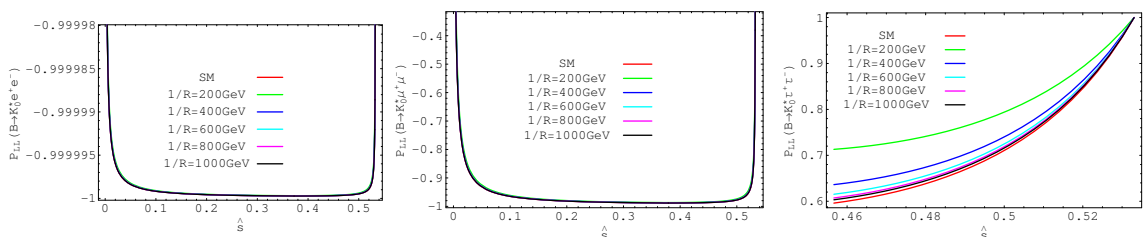**Figure 7**. The same as figure 2, but for $P_{NN}$ polarization.



**Figure 8**. The dependence of the $P_{LL}$ polarization of the $B \to K_0^* l^+ l^-$ on $\hat{s}$ at different fixed values of $1/R$ and the SM for different leptons.

factor, $1/R$ at different fixed values of $\hat{s}$ and different leptons are shown in figures 2–7. A quick glance at these figures leads to the following conclusions:

- As it is expected, all polarization asymmetries lie between $-1$ and $1$. There are also discrepancies between the predictions of two models for small $1/R$ values, except the $P_{LL}$, $P_{LN}$ and $P_{NT}$ for $e$ and $\mu$ cases for which the differences between the ACD and SM models are very small. At high values of $1/R$, two models have approximately the same predictions.

- All double-lepton polarization asymmetries have the same sign for all leptons, except the $P_{LL}$ at which the sign for the $\tau$ mode is different than those for the $e$ and $\mu$ cases.

- In contrast with the branching ratios, some of the polarization asymmetry predictions are different for the $e$ and $\mu$ cases.

- In $P_{NN}$ for $e$ and $\mu$ and $P_{TT}$ for $e$, the SM gives zero for $\hat{s} = 0.5$, while we see considerable nonzero values for them in ACD model at low $1/R$ values.

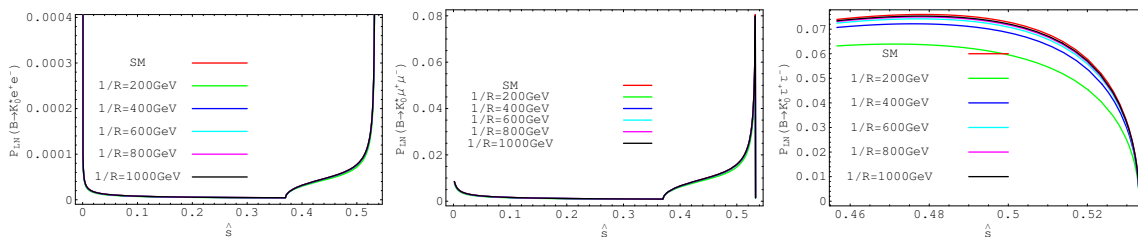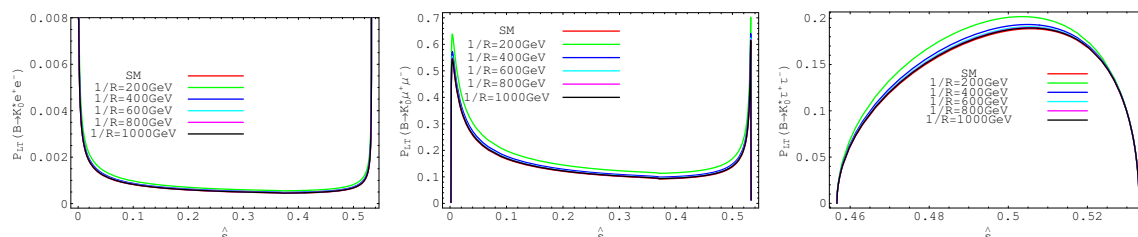**Figure 9**. The same as figure 8, but for $P_{LN}$ polarization.



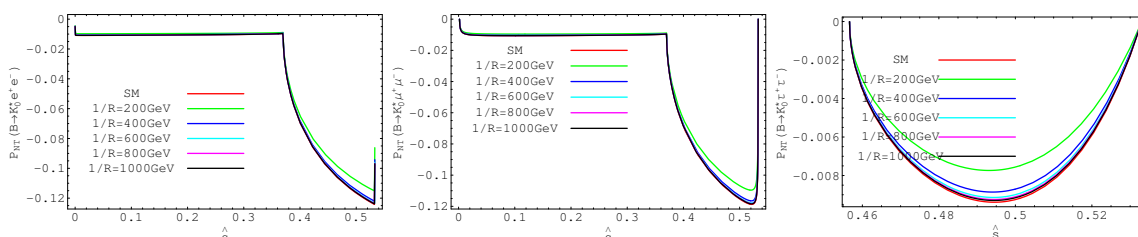**Figure 10**. The same as figure 8, but for $P_{LT}$ polarization.



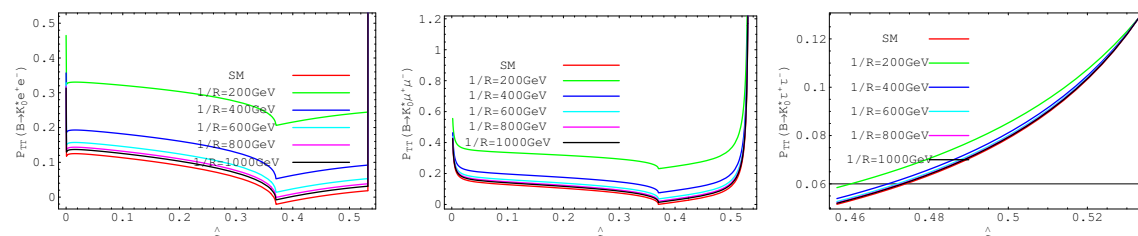**Figure 11**. The same as figure 8, but for $P_{NT}$ polarization.



**Figure 12**. The same as figure 8, but for $P_{TT}$ polarization.

We depict the dependence of the different double-lepton polarization asymmetries on $\hat{s}$ at different fixed values of $1/R$ and the SM for different leptons in figures 8–13. From these figures, we infer the following information:

- The longitudinal-longitudinal polarization asymmetry, $P_{LL}$, remains approximately unchanged in whole physical region except the end points for the $e$ and $\mu$. This asymmetry grows as $\hat{s}$ increases and reaches its maximum at the upper bound of the allowed physical region for $\tau$.
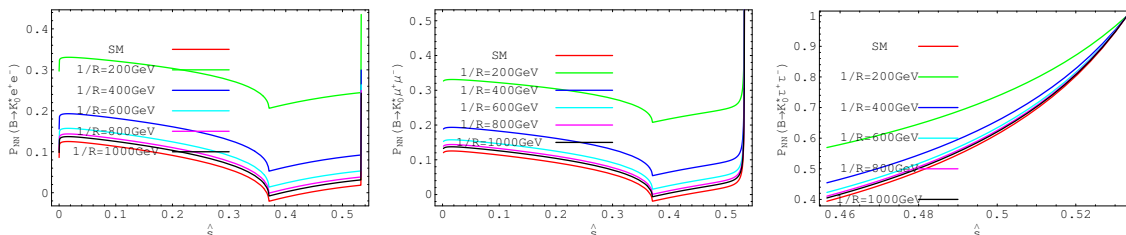
**Figure 13**. The same as figure 8, but for $P_{NN}$ polarization.

- The $P_{LN}$ is zero in the interval, $4\hat{m}_l^2 \leq \hat{s} \leq 0.37$, but after $\hat{s} = 0.37$ it starts to increase up to the upper limit for $\hat{s}$ $((1 - \hat{m}_{K_0^*})^2)$ for $e$ and $\mu$. For $\tau$ case, this asymmetry remains approximately unchanged in the interval $4\hat{m}_l^2 \leq \hat{s} \leq 0.50$, but after this point it starts to diminish and becomes zero at the endpoint.

- The $P_{LT}$ slightly decreases as $\hat{s}$ increases for the $e$ and $\mu$ cases and has a very small value for the $e$ case compared to that of the $\mu$. This asymmetry for $\tau$, first increases then it decreases after reaching a maximum as $\hat{s}$ increases in the allowed physical region.

- The normal-transversal polarization asymmetry, $P_{NT}$ remain also unchanged in the interval, $4\hat{m}_l^2 \leq \hat{s} \leq 0.37$, for $e$ and $\mu$, but it grows after this interval and has negative sign. In the case of $\tau$, this asymmetry also has negative sign and it increases to reach a maximum then decreases as $\hat{s}$ increases.

- For the $e$ and $\mu$, the $P_{TT}$ and $P_{NN}$ start to decrease as $\hat{s}$ increases. The values of these asymmetries in the SM and higher values of the compactification factor become zero around $\hat{s} = 0.37$ then they start to increase as $\hat{s}$ increases. They have minimums at low $1/R$ values at the same $\hat{s}$. For $\tau$ case, the $P_{TT}$ and $P_{NN}$ grow as $\hat{s}$ increases and the $P_{NN}$ reaches its maximum at the upper bound.

At the end of this section, we would like to quantify the uncertainties of our predictions associated with the errors of the hadronic form factors. In this connection, we show the dependence of the differential branching ratios for $\mu$ and $\tau$ on $\hat{s}$ in figure 14 and dependence of $P_{LL}$, $P_{TT}$ and $P_{NN}$ on $\hat{s}$ only for $\mu$ in figure 15. These figures contain our predictions (a) in ACD model at $1/R = 200\,GeV$ when the errors presented in table 1 are added to the central values of the form factors, (b) the same model and $1/R$, but when the errors of form factors are subtracted from the central values and (c) in SM when central values of the form factors are considered. From figure 14, we see that the results of SM lies between the cases (a) and (b) but close to the case (b). In the case of $\mu$, the maximum deviation from the SM is in lower values of $\hat{s}$ and belongs to the case (a) and has the value about two times grater than that of the SM. For $\tau$ case, the maximum deviation of the ACD prediction lies at middle of the allowed physical region for the $\hat{s}$. At this point, the ACD prediction in the case (a) is approximately six times greater than the SM prediction. The similar deviations from the SM model has also been observed for instance in [20] for $\Lambda_b \to \Lambda l^+ l^-$, but at higher values of $\hat{s}$. figure, 15 depicts an interesting observation. The ACD model in
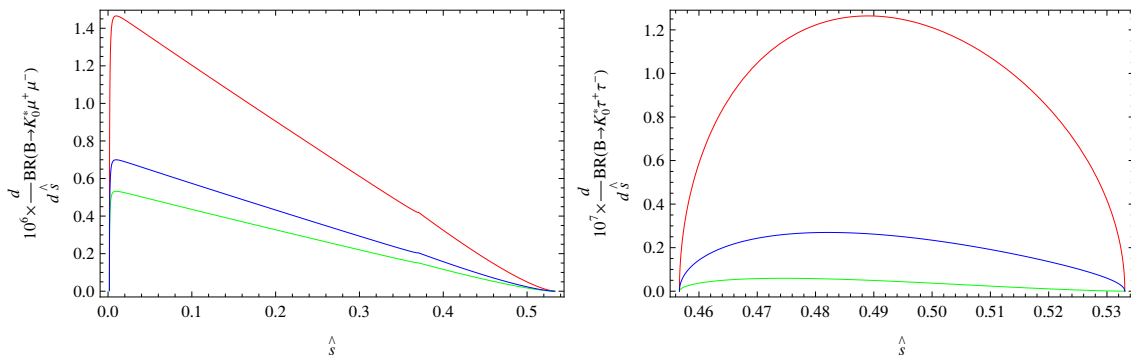
**Figure 14**. The dependence of differential branching ratio for $\mu$ and $\tau$ on $\hat{s}$. The red color shows the results at $1/R = 200\,GeV$ when the errors of form factors are added to the central values, the green one shows the predictions at the same value of $1/R$, but when the errors are subtracted from the central values and the blue color shows the result of the SM, when the central value of the form factors are considered
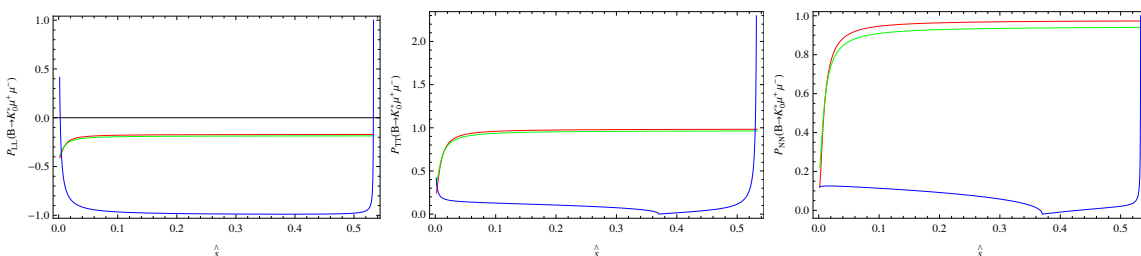


**Figure 15**. The same as figure 14, but for $P_{LL}$, $P_{TT}$ and $P_{NN}$ polarizations and only for $\mu$.

the cases (a) and (b) has approximately the same predictions, but ignoring the end points at which two models have same predictions, the ACD model predictions are 1/5, 5 and approximately 9 times of the SM predictions for $P_{LL}$, $P_{TT}$ and $P_{NN}$, respectively.

## 4 Conclusion

We have calculated some observables such as the branching ratio and double-lepton polarization asymmetries associated with the $B \to K_0^*(1430)l^+l^-$ channel in the framework of the ACD model with a single universal extra dimension. We discussed the sensitivities of these observables to the compactification parameter, $1/R$. We compared the results obtained from the ACD model with the predictions of the standard model. The predictions of the two models approach each other at around $1000\,GeV$ for the value of the compactification parameter, $1/R$. However the results for the two models differ significantly at lower values of the compactification parameter. This difference grows specially when the errors of the form factors calculated from the QCD sum rules in table 1 are taken into account. The maximum deviation from the predictions of SM for the considered quantities, obtained using the central values of form factors, belongs to the case of ACD model predictions, where the errors of the form factors are added to the central values of the form factors. This deviation also increases as $1/R$ decreases, such that at low $1/R$, the discrep-

ancy between predictions of the SM and ACD models reaches to approximately one order of magnitude for some observables. These results beside the other evidences for deviation of the ACD model predictions from the SM obtained via investigating many observables related to the $B$ and $\Lambda_b$ channels, which due to the heavy bottom quark have large range of $q^2$, in [6, 7, 9, 11–14, 20–26], can be considered as a signal for the existence of extra dimensions in the nature which should we search for in the experiments.

The order of magnitude for the branching ratio shows a possibility to study $B \to K_0^*(1430)l^+l^-$ channel at the LHC. Any measurements on the branching ratio as well as the double-lepton polarization asymmetries and determination of their signs and their comparison with the obtained results in this paper can give valuable information about the nature of the scalar meson $K_0^*(1430)$ as well as the possible extra dimensions.

## References

[1] N. Arkani-Hamed, S. Dimopoulos and G.R. Dvali, *The hierarchy problem and new dimensions at a millimeter*, *Phys. Lett.* **B 429** (1998) 263 [hep-ph/9803315] [SPIRES].

[2] N. Arkani-Hamed, S. Dimopoulos and G.R. Dvali, *Phenomenology, astrophysics and cosmology of theories with sub-millimeter dimensions and TeV scale quantum gravity*, *Phys. Rev.* **D 59** (1999) 086004 [hep-ph/9807344] [SPIRES].

[3] I. Antoniadis, N. Arkani-Hamed, S. Dimopoulos and G.R. Dvali, *New dimensions at a millimeter to a Fermi and superstrings at a TeV*, *Phys. Lett.* **B 436** (1998) 257 [hep-ph/9804398] [SPIRES].

[4] I. Antoniadis, *A Possible new dimension at a few TeV*, *Phys. Lett.* **B 246** (1990) 377 [SPIRES].

[5] T. Appelquist, H.-C. Cheng and B.A. Dobrescu, *Bounds on universal extra dimensions*, *Phys. Rev.* **D 64** (2001) 035002 [hep-ph/0012100] [SPIRES].

[6] A.J. Buras, M. Spranger and A. Weiler, *The Impact of Universal Extra Dimensions on the Unitarity Triangle and Rare K and B Decays*, *Nucl. Phys.* **B 660** (2003) 225 [hep-ph/0212143] [SPIRES].

[7] A.J. Buras, A. Poschenrieder, M. Spranger and A. Weiler, *The impact of universal extra dimensions on $B \to X/s$ gamma, $B \to X/s$ gluon, $B \to X/s$ $\mu^+\mu^-$, $K(L) \to pi0$ $e^+e^-$ and $\epsilon'/\epsilon$*, *Nucl. Phys.* **B 678** (2004) 455 [hep-ph/0306158] [SPIRES].

[8] A.J. Buras and M. Münz, *Effective Hamiltonian for $B \to X(s)$ $e^+e^-$ beyond leading logarithms in the NDR and HV schemes*, *Phys. Rev.* **D 52** (1995) 186 [hep-ph/9501281] [SPIRES].

[9] P. Colangelo, F. De Fazio, R. Ferrandes and T.N. Pham, *Exclusive $B \to K(*)$ $\ell^+\ell^-$, $B \to K(*)$ nu anti-nu and $B \to K*$ gamma transitions in a scenario with a single universal extra dimension*, *Phys. Rev.* **D 73** (2006) 115006 [hep-ph/0604029] [SPIRES].

[10] T. Appelquist and H.-U. Yee, *Universal extra dimensions and the Higgs boson mass*, *Phys. Rev.* **D 67** (2003) 055002 [hep-ph/0211023] [SPIRES].

[11] V. Bashiry, M. Bayar and K. Azizi, *Double-lepton polarization asymmetries and polarized forward backward asymmetries in the rare $b \to s\ell^+\ell^-$ decays in a single niversal extra dimension scenario*, *Phys. Rev.* **D 78** (2008) 035010 [arXiv:0808.1807] [SPIRES].

[12] M.V. Carlucci, P. Colangelo and F. De Fazio, *Rare $B_s$ decays to $\eta$ and $\eta'$ final states*, *Phys. Rev.* **D 80** (2009) 055023 [arXiv:0907.2160] [SPIRES].

[13] T.M. Aliev, M. Savci and B.B. Sirvanli, *Double-lepton polarization asymmetries in Lambda/b → Lambda $\ell^+\ell^-$ decay in universal extra dimension model*, *Eur. Phys. J.* **C 52** (2007) 375 [hep-ph/0608143] [SPIRES].

[14] I. Ahmed, M.A. Paracha and M.J. Aslam, *Exclusive $B \to K_1 l^+l^-$ decay in model with single universal extra dimension*, *Eur. Phys. J.* **C 54** (2008) 591 [arXiv:0802.0740] [SPIRES].

[15] M. Misiak, *The $b \to s\, e^+e^-$ and $b \to s\, gamma$ decays with next- to-leading logarithmic QCD corrections*, *Nucl. Phys.* **B 393** (1993) 23 [SPIRES].

[16] T.M. Aliev, K. Azizi and M. Savci, *Analysis of rare ($B \to K_0*(1430)l^+l^-$ decay) within QCD sum rules*, *Phys. Rev.* **D 76** (2007) 074017 [arXiv:0710.1508] [SPIRES].

[17] T.M. Aliev, V. Bashiry and M. Savci, *Double-lepton polarization asymmetries in the $B \to K$ $\ell^+\ell^-$ decay beyond the standard model*, *Eur. Phys. J.* **C 35** (2004) 197 [hep-ph/0311294] [SPIRES].

[18] V. Bashiry, S.M. Zebarjad, F. Falahati and K. Azizi, *The effects of fourth generation on the double lepton polarization in $B \to K\ell^+\ell^-$ decay*, *J. Phys.* **G 35** (2008) 065005 [arXiv:0710.2619] [SPIRES].

[19] S. Fukae, C.S. Kim and T. Yoshikawa, *A systematic analysis of the lepton polarization asymmetries in the rare B decay, $B \to X/s\ tau+\ tau-$*, *Phys. Rev.* **D 61** (2000) 074015 [hep-ph/9908229] [SPIRES].

[20] Y.-M. Wang, M.J. Aslam and C.-D. Lu, *Rare decays of $\Lambda_b \to \Lambda\gamma$ and $\Lambda_b \to \Lambda l^+l^-$ in universal extra dimension model*, *Eur. Phys. J.* **C 59** (2009) 847 [arXiv:0810.0609] [SPIRES].

[21] P. Colangelo, F. De Fazio, R. Ferrandes and T.N. Pham, *Spin effects in rare $B \to X/s\ tau+ tau-$ and $B \to K* tau+ tau-$ decays in a single universal extra dimension scenario*, *Phys. Rev.* **D 74** (2006) 115006 [hep-ph/0610044] [SPIRES].

[22] P. Colangelo, F. De Fazio, R. Ferrandes and T.N. Pham, *FCNC $B_s$ and $Lambda_b$ transitions: Standard model versus a single universal extra dimension scenario*, *Phys. Rev.* **D 77** (2008) 055019 [arXiv:0709.2817] [SPIRES].

[23] U. Haisch and A. Weiler, *Bound on minimal universal extra dimensions from anti-B → X/s gamma*, *Phys. Rev.* **D 76** (2007) 034014 [hep-ph/0703064] [SPIRES].

[24] R. Mohanta and A.K. Giri, *Study of FCNC mediated rare $B_s$ decays in a single universal extra dimension scenario*, *Phys. Rev.* **D 75** (2007) 035008 [hep-ph/0611068] [SPIRES].

[25] G. Devidze, A. Liparteliani and U.-G. Meissner, *$B_{s,d} \to \gamma\gamma$ decay in the model with one universal extra dimension*, *Phys. Lett.* **B 634** (2006) 59 [hep-ph/0510022] [SPIRES].

[26] I.I. Bigi, G.G. Devidze, A.G. Liparteliani and U.G. Meissner, *$B \to \gamma\gamma$ in an ACD model*, *Phys. Rev.* **D 78** (2008) 097501 [arXiv:0806.1541] [SPIRES].